Available online at www.sciencedirect.com
SCIENCE DIRECT
Biochimica et Biophysica Acta 1741 (2005) 173 – 182
BIOCHIMICA ET BIOPHYSICA ACTA
BBA
http://www.elsevier.com/locate/bba

Cardiac volume overload rapidly induces oxidative stress-mediated myocyte apoptosis and hypertrophy

C. Fiorillo[a,*,1], C. Nediani[a,1], V. Ponziani[a], L. Giannini[a], A. Celli[a], N. Nassi[a], L. Formigli[b], A.M. Perna[c], P. Nassi[a]

[a]*Department of Biochemical Sciences, Viale Morgagni 50, 50134 Florence, Italy*
[b]*Department of Human Anatomy and Histology, Viale Morgagni 85, 50134 Florence, Italy*
[c]*Department of Experimental Surgery, Viale Morgagni 85, 50134 Florence, Italy*

Received 14 October 2004; received in revised form 17 February 2005; accepted 21 March 2005
Available online 28 April 2005

Abstract

Oxidative stress stimulates both growth and apoptosis in cardiac myocytes in vitro. We investigated the role of oxidative stress in the initial phases of cardiac remodeling induced in an animal model by volume overload. As plausible candidates for a connection between oxidative stress and cardiomyocyte apoptosis or hypertrophy, we explored the behaviour of two MAPKs, specifically JNK and ERK. At 48 h of overload, the greatest increase in oxidative stress coincided with a peak of cardiomyocyte apoptosis. This was possibly induced through the mitochondrial metabolism, as evidenced by the release of cytochrome *c* and a significant increase in the active forms of caspase-9 and -3, but not caspase-8. Oxidative stress markers significantly decreased at 96 h of overload, combined with a marked attenuation of apoptosis and the appearance of hypertrophy. The highest levels of JNK and the lowest levels of ERK phosphorylation were observed at 48 h of overload. Conversely, a sharp increase in ERK phosphorylation was detected at 96 h of overload coinciding with the hypertrophic response. Together these results show that oxidative stress is an early and transient event in myocardial volume overload. They suggest that oxidative stress mediates amplitude dependent apoptotic and hypertrophic responses in cardiomyocytes through the selective activation of, respectively, JNK and ERK.

Keywords: Oxidative stress; Cardiac volume overload; Apoptosis; Hypertrophy; MAPKs

1. Introduction

Volume overload is a major cause of myocardial remodeling (MR), a process linked closely to the development of heart failure. MR is characterized by progressive morphological and functional alterations, specifically changes in chamber geometry and impairment of pump function. At the cellular level, MR involves modifications of interstitial matrix turnover by cardiac fibroblasts, myocyte hypertrophy, and myocyte loss, chiefly by apoptosis. Although many factors, including neurohormones, cytokines, and growth factors, have been proposed as connecting these cellular events to the mechanical strain induced by volume overload [1], experimental evidence increasingly indicates a central role of oxidative stress. Several recent reports demonstrate that reactive oxygen species (ROS) regulate the phenotype of cardiomyocytes and that oxidative stress, due to an increased generation of ROS and eventually to an impairment of antioxidant defences, is a possible mediator of both cell death and growth [2,3]. A plausible explanation for such different effects is the magnitude of the increase in ROS concentration [4]. Siwik et al. [5] found that graded increases in cardiomyocyte oxidative stress, induced through the inhibition of (Cu, Zn) superoxide dismutase by the copper chelator diethyldithiocarbamic acid

* Corresponding author. Tel.: +39 55 413765; fax: +39 55 4222725.
E-mail address: claudia.fiorillo@unifi.it (C. Fiorillo).
[1] C. Fiorillo and C. Nediani contributed equally to this work.

0925-4439/$ - see front matter © 2005 Elsevier B.V. All rights reserved.
doi:10.1016/j.bbadis.2005.03.015

(DDC), resulted in two distinct responses. Low DDC concentrations, which induced moderate oxidative stress (with 40% increase in ROS production over control), stimulated protein synthesis and myocyte hypertrophy. Conversely, high DDC concentrations caused larger increases in ROS production and led to myocyte apoptosis. Other studies have shown a relationship between myocardial mechanical strain (as occurs in volume overload) and oxidative stress. Pimentel et al. [6] reported that mechanical stretching of myocytes causes an amplitude-dependent increase in ROS production, which is associated with different phenotypic effects. Low levels of ROS production, observed in cardiomyocytes stretched at low amplitude, correlate with fetal gene expression and hypertrophy, while high amplitude stretch levels induce higher ROS production and apoptosis.

In spite of progress in understanding the cellular mechanisms of MR, the exact order of events between myocyte stimulation, generation of ROS, and induction of specific phenotypes remains to be elucidated [4]. One possible means to distinguish between the two different responses to oxidative stress (hypertrophy and apoptosis) may be attributed to the redox-sensitive, mitogen activated protein kinases (MAPKs) [6,7]: c-Jun NH_2 terminal protein kinase (JNK) is a leading candidate for the transduction mechanisms that transmit and convert stress signaling into apoptosis, and extracellular signal-regulated kinase (ERK) seems to have an antiapoptotic role and be involved in cell growth processes. Different ROS levels might selectively activate these kinases leading to apoptosis or, alternatively, to myocyte hypertrophy.

Considering that most studies on MR have focused on late changes, the present investigation examines the initial phases of MR in an animal model of cardiac acute volume overload. We explored the occurrence of oxidative stress, its relationship with cardiomyocyte apoptosis and hypertrophy, and possible molecular mechanisms to account for these processes.

2. Materials and methods

2.1. Experimental model

The experimental protocol described in the study conforms with the *Guide for the Care and Use of Laboratory Animals* published by the US National Institutes of Health (NIH Publication No. 85-23, revised 1996). Twenty farm pigs (Landrace), aged 2–3 months, weighing 30–45 kg were randomly divided in four groups: a group of sham-operated controls ($n=5$) and three groups undergoing aortacaval shunt for respectively 24, 48, 96 h ($n=5$ for each group). Animals, fasting overnight, were premedicated with intramuscular ketamine (15 mg/kg) and diazepam (1 mg/kg). Anesthesia was induced with ketamine (0.5 mg/kg) and atropine (0.5 mg/kg) given intravenously through an ear vein. Pigs were subsequently oro-tracheally intubated and ventilated with oxygen supplemented with 50% N_2O and fluothane at 1–1.5%. Pancuronium bromide (0.1 mg/kg) was given at the beginning of the surgical procedure. The abdomen was opened via a midline incision, and the inferior part of the vena cava and abdominal aorta distal to the renal arteries were cleaned of fat and adventitia. The shunt was performed using a Dacron prosthesis (8-mm diameter) which was sutured latero-laterally to the abdominal aorta and to the inferior vena cava using partial occluding clamps. When the anastomosis was completed, the clamps were released, hemostasis was obtained and the abdomen was closed. At 24, 48, and 96 h after surgery, the animals were again anesthetized, subjected to hemodynamic measurements and then sacrificed using humanitarian methods. After the sacrifice the heart was removed by a midline sternotomy and specimens of left ventricle (LV) tissue were taken for biochemical and histological studies. Sham operated animals underwent an identical procedure (laparotomic incision followed by the hemodynamic and echocardiographic evaluations) except for aortacaval shunt.

2.2. Hemodynamic and echocardiographic measurements

Hemodynamic and echocardiographic measurements were performed with the animal under general anesthesia. A 6F pigtail catheter was introduced into the left femoral artery and advanced to monitor left ventricular and descending aortic pressure. A Swan–Ganz catheter was advanced from an external jugular vein to the pulmonary artery to measure pulmonary capillary wedge pressure and cardiac output (thermodilution). Two dimensional and M-mode echocardiographic studies (2.25/3.5 MHz transducer, SIM 5000) and relative measurements were performed on the right parasternal area and recorded on videotape [8]; wall thicknesses were measured according to the recommendations of the American Society for Echocardiography [9]. Left ventricular mass (LVM) was calculated using a validated formula [10]. Measurements were analyzed independently by two experienced echocardiographers. Inter-observer and intra-observer variabilities were $4.1\pm0.5\%$ and $2.5\pm0.3\%$ for cavity size and $3.7\pm0.4\%$ and $2.1\pm0.3\%$ for wall thickness, respectively.

2.3. Preparation of homogenates

100 mg of myocardium samples were incubated for 1 h at 37 °C in phosphate buffered saline containing 0.1% collagenase type 1. The mixture was centrifuged at $100\times g$ for 15 min and the pellet was homogenized (20% wt/vol with a glass-glass Potter-Elvejhem homogenizer) in ice-cold 20 mM Tris–HCl (pH 8) buffer containing 2 mM EDTA, 1% Triton X-100, 10% glycerol, 137 mM NaCl, 6 M Urea, 0.2 mM PMSF and 10 μg/ml of aprotinin and leupeptin. The homogenate was then sonicated and centrifuged at $10{,}000\times g$ for 10 min. The resulting supernatant

was used for estimation of lipoperoxidation, protein carbonyl content, and total antioxidant capacity (TAC). Total homogenate, omitting the incubation step with collagenase type I, was used for caspase-3, caspase-8, caspase-9, JNK, and ERK determinations. Protein concentration was assayed according to the method of Bradford [11].

2.4. Purification of subcellular fractions (nuclei, cytosol, mitochondria)

Subcellular fractionation was achieved using a cytosol/mitochondria fractionation kit (Oncogene research products, San Diego, CA, USA). Nuclear fractionation was used to determine PARP activity. Cytosolic and mitochondrial fractions were isolated to assess cytochrome *c* compartmentalization. Complete separation of nuclear, mitochondrial and cytosolic fractions was assessed by immunoblotting using anti-histone (Chemicon Int. Temecula, CA), anti-cytochrome oxidase (COX) subunit IV (Molecular Probes, Eugene, OR, USA), and anti-β tubulin (Santa Cruz Biotech, Santa Cruz, CA, USA) antibodies. The immunoblotting with these antibodies helped to verify that equal amounts of proteins were loaded on the lanes.

2.5. Measurement of lipid peroxidation products

To assess the rate of lipid peroxidation, malonaldehyde (MDA) and 4-hydroxyalkenals (4-HNE) concentrations were determined by a colorimetric method based on the reaction of a chromogenic reagent, N-methyl-2-phenyl-indole, with MDA or 4-HNE at 45 °C [12].

2.6. Determination of protein carbonyls

The protein carbonyl content was determined using the 2,4-dinitrophenylhydrazine method of Levine et al. [13]. 200 μg of supernatant proteins were dried in a vacuum centrifuge, and 500 μl of 10 mM 2,4-dinitrophenylhydrazine in 2 M HCl was added to each tube. Spectrophotometric measurement was made at 375 nm, using 22,000 M^{-1} cm^{-1} as the molar absorption coefficient.

2.7. Total antioxidant capacity (TAC) assay

TAC (Total Antioxidant Status, Randox, UK) was assayed using a spectrophotometric method. 2,2′-azino-di-[3-ethylbenzthiazoline sulphonate] (ABTS) was incubated with a peroxidase (metmyoglobin) and H_2O_2 to produce the radical cation ABTS•+. This has a relatively stable blue-green color, which absorbs at 600 nm. Antioxidants contained in the sample suppress this color production to an extent proportional to their concentration. The results are calculated using a reference curve based on the soluble antioxidant Trolox (6-hydroxy-2,5,7,8-tetramethylchroman-2-carboxylic acid) as a standard.

2.8. Poly(ADP-ribose)polymerase (PARP) activity measurement

PARP activity was assessed by immunodot blot which detects poly(ADP-ribosylated) proteins [14]. An aliquot of nuclear suspension was diluted in 0.4 M NaOH containing 10 mM EDTA and loaded onto a Hybond N+ nylon membrane (Amersham, Life Science, England). The membrane was washed once with 0.4 M NaOH, blocked in PBS-MT (PBS, pH 7.4, containing 5% not fat dried milk and 0.1% Tween 20) and then incubated overnight with the primary antibody LP98-10 (Alexis, San Diego, USA). The membrane was washed with PBS-MT and incubated for 30 min with peroxidase-conjugated anti-rabbit IgG (Amersham, Life Science). The blot was again washed with PBS-MT followed by washes in PBS prior to analysis by chemiluminescence. Image analysis of the dot blot was performed with Quantity One software (Bio-RAD Laboratories, Milano, IT). The membrane was subsequently immunoblotted with anti-histone antibodies to verify that equal amounts of proteins were loaded.

2.9. Caspase-3 activity measurement

Aliquots of the homogenate fractions derived from the above-described procedure were centrifuged at $22000 \times g$ and 4 °C for 10 min. The resulting supernatant was used for the measurement of caspase-3 (DEVDase) activity by the colorimetric CaspACE assay system, (Promega, WI, USA). Positive control was obtained by staurosporine-induction of apoptosis in cultured rat cardiomyocytes as according to Yue T.L. et al [15]. Cells were harvested by centrifugation at $450 \times g$ for 10 min at 4 °C and after washing with PBS were resuspended in cell lysis buffer. Cell lysates were centrifuged at $15{,}000 \times g$ for 20 min at 4 °C and the supernatant fraction was collected as a cell extract. The colorimetric substrate (Ac-DEVD-pNA) is labeled with the chromophore p-nitroaniline (pNA), which is released from the substrate upon cleavage by DEVDase. Free pNA produces a yellow color that is monitored by photometer at 405 nm. Activity is expressed as nmol of pNA released/h/mg protein.

2.10. Western blot

Equal protein amounts of total homogenate (or mitochondrial and cytosolic fractions in the case of cytochrome *c*), determined by the method of Bradford, were diluted in Laemmli's sample buffer, boiled for 5 min and separated on 15% SDS-PAGE. Proteins were transferred to PVDF hybond membranes (Millipore Corporation, Billerica, MA, USA). An equal rate of transfer among lanes was confirmed by reversible staining with Ponceau S (Sigma, Milano, IT). The membranes were then incubated with (rabbit) anti caspase-3/CPP32 antibody (Biosource International, CA, USA), (rabbit) anti-caspase-8 (Chemicon Int. Temecula, CA, USA), (rabbit) anti-caspase-9 antibody (Santa Cruz Biotech,

Table 1
Hemodynamic and echocardiographic changes after aortacaval shunt

Hours	0	24	48	96
Heart rate (beats/min)	82±5	111±8*	108±8*	107±7*
Aortic systolic pressure (mm Hg)	125±18	115±4*	116±7	117±7
PWP (mm Hg)	14±4	23±4*	25±5*	21±4*
Cardiac output (ml/min)	2009±463	3549±888*	3370±503*	3519±203*
LVESP (mm Hg)	127±23	121±11	123±5	124±7
LVEDP (mm Hg)	8±2	14±2*	15±2*	10±2
DWT (mm)	7.8±0.7	8.0±0.9	7.9±0.9	8.1±0.6
SWT (mm)	11.2±1.0	11.1±0.3	11.1±1.2	11.4±1.1
LVM (g/kg)	2.39±0.3	2.71±0.2	3.01±0.5	3.15±0.4*

Values are means±S.D. ($n=5$ for each group.)
LVESP, left ventricular end-systolic pressure; LVEDP, left ventricular end-diastolic pressure; DWT, diastolic wall thickness; SWT, systolic wall thickness; LVM, left ventricular mass; PWP, pulmonary wedge pressure.
* Significantly different ($P<0.05$) vs. Control.

Santa Cruz, Ca, USA), (mouse) anti-cytochrome *c* (Oncogene Research Products, San Diego, CA, USA), incubation was overnight at 4 °C. After washing, the membranes were incubated with peroxidase-conjugated secondary antibodies for 1 h before immunolabeled bands were detected using a SuperSignal West Dura (Pierce, Rockford, IL, USA). Control values were taken as 100%, and the experimental samples were calculated as a percentage of the control within the same blot. Tubulin (for homogenate) or cytochrome oxidase (COX) subunit IV (for mitochondria) was used to control for equal protein loading.

Activation of JNK and ERK MAPKs was assessed by Western blotting, as described above, with antibodies that specifically recognize the phosphorylated, active forms of these kinases, using (mouse) anti p-JNK and (rabbit) anti p-ERK (Thr202/Tyr204), (Cell Signalling Technology, Inc Beverly MA, USA). Rabbit anti JKN and ERK antibodies (Santa Cruz Biotech, Santa Cruz, Ca, USA) were used to detect their total levels.

2.11. Evaluation of apoptosis

In situ end labeling of nicked DNA (ISEL assay) was performed on paraffin-embedded sections, as reported previously [16]. After treatment with 2 mg/ml proteinase K to remove excess protein from the nuclei, the tissue sections were incubated with the Klenow fragment of DNA polymerase I and biotinylated deoxynucleotides (FRAGEL-Klenow, DNA fragmentation kit, Calbiochem, CA) in a humidified chamber at 37 °C for 90 min. The sections were then incubated with streptavidin-peroxidase for 10 min and stained with diaminobenzidine tetrahydrochloride (DAB). Counterstaining was performed with methyl green. Viable non-apoptotic nuclei appeared green-stained. Apoptotic nuclei were easily recognized by a dark brown staining, in contrast to necrotic and mitotic cells which were weakly stained. The number of ISEL-positive cardiomyocytes was counted in at least five different microscopic fields for each section, containing approximately 200 cardiomyocytes/section obtained from each animal of the different experimental group. The quantitative analyses were performed by two different persons blinded to the experimental protocol and the individual values were then averaged. The cardiomyocyte nuclei were identified by standard morphological criterion such as the typical ovoid nucleus included in the striated cytoplasm of myocardial fibers.

2.12. Measurement of cell size

Additional sections from paraffin-embedded tissue were stained with 1% Toluidine-blue. Ten myocytes from 6 randomly selected optical fields in each transversely sectioned specimen (3 from each animal) of 26300 μm^2 were collected at a 40× by the Adobe Photoshop Program. The area of individual cells containing well defined round nuclei was measured using the Scion Image Program.

2.13. Statistical analysis

All data are expressed as mean±standard deviation (SD). Comparisons between the different groups were performed by ANOVA followed by Bonferroni *t*-test. A P value < 0.05 was accepted as statistically significant.

3. Results

3.1. Hemodynamic and echocardiographic data

During the study period, the aortacaval shunt remained pervious in all the operated pigs and no animal showed signs of heart failure or died within 96 h after surgery. As reported in Table 1, the presence of a consistent imposed overload was confirmed by the increase in cardiac output observed 24 h after the shunt. No significant modifications were observed for left ventricular end systolic pressure (LVESP), while left ventricular end diastolic pressure (LVEDP) increased significantly from 24 h to 48 h of overload, and returned to the control value at 96 h. Pulmonary wedge pressure exhibited changes similar to those observed for LVEDP, except that at 96 h, it was still elevated. After 96 h from surgery, the overloaded hearts appeared to develop a hypertrophic

Table 2
Oxidative stress markers and antioxidant capacity in overloaded hearts

	MDA+4-HNE (nmol/mg protein)	Protein carbonyls (nmol/mg protein)	Total antioxidant capacity (pmol/mg protein)
Control	4.06±0.35	4.31±0.73	25.3±1.41
24 h overload	5.30±0.33	6.62±0.95	24.7±1.82
48 h overload	8.98±0.35*	10.05±1.22*	18.5±1.33*
96 h overload	7.02±0.28[a,*]	8.47±1.92*	26.1±1.52

[a] Significantly different ($P<0.05$) vs. 48 h.
* Significantly different ($P<0.05$) vs. Control.

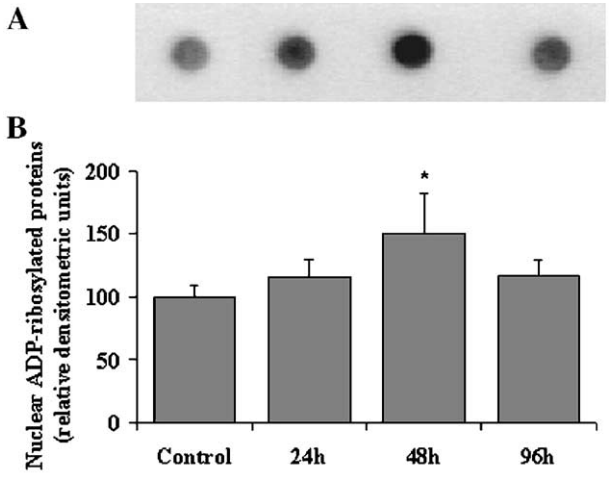

Fig. 1. Immunodot blot of ADP-ribosylation levels of PARP nuclear substrates. (A) Representative dot blot showing poly(ADP-ribosylation) (PAR) level of nuclear proteins in control and volume-overloaded hearts. (B) Quantitative data. Each bar represents the mean±S.E.M. of five different blots. Signals were quantified by densitometric analysis and are expressed as a percentage of the control. *Significant difference ($P<0.05$) from control.

response, since their LVM was significantly higher with respect to the control value. During the study period, systolic and diastolic wall thickness were not different between the groups. Probably, the period of observation was not long enough to detect significant modifications in these parameters, all the more so since volume overload is known to induce enlargements in cardiac cavities, but only little changes in ventricular wall thickness.

3.2. Oxidative stress markers

Lipid peroxidation products, protein carbonyl content, and total antioxidant capacity were measured to assess the occurrence and intensity of oxidative stress under these experimental conditions. Table 2 shows that the levels of MDA and 4-HNE, which are typical stable end products of the lipoperoxidative process, had significantly increased at 48 h and 96 h relative to the control value. In addition, at 96 h of overload, the concentration of these markers was significantly reduced when compared to the 48-h value. Protein carbonyl content showed a similar time course reaching significance at 48 and 96 h. As for total antioxidant capacity, assayed as an index of antioxidant defences, we found a significant decrease at 48 h of overload, consistent with the maximal levels of oxidative stress markers (Table 2).

PARP activity, which is triggered by DNA strand breaks and may represent an indirect marker of free radical-induced genomic damage, was enhanced in the overloaded hearts. The most marked and significant increase (about 50% above the control value) was observed at 48 h, consistent with other findings that this is the time of greatest oxidative stress (Fig. 1).

3.3. Cardiomyocyte apoptosis and hypertrophy

The ISEL procedure, which detects apoptotic DNA fragmentation, was used to investigate whether oxidative stress is linked to the occurrence of cardiomyocyte apoptosis in our volume overloaded hearts. Quantitative analysis for the number of nuclei staining positive for ISEL (dark brown) showed a wave of apoptosis which peaked at 48 h after

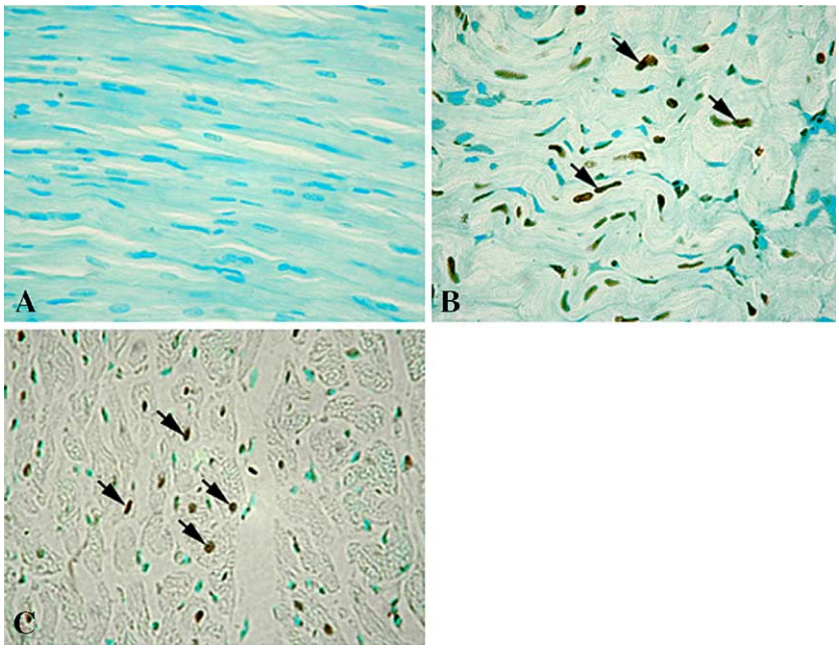

Fig. 2. Detection of apoptotic nuclei by ISEL technique. Representative LM images of control (A) and 48 h volume overloaded heart (B, longitudinal and C, transversal sections). Note that some cardiomyocytes (arrows) exhibit dark-brown ISEL-positive nuclei in the overloaded myocardium, whereas cells with apoptotic nuclear fragmentation are absent in the control myocardium. Viable non apoptotic nuclei appeared green.

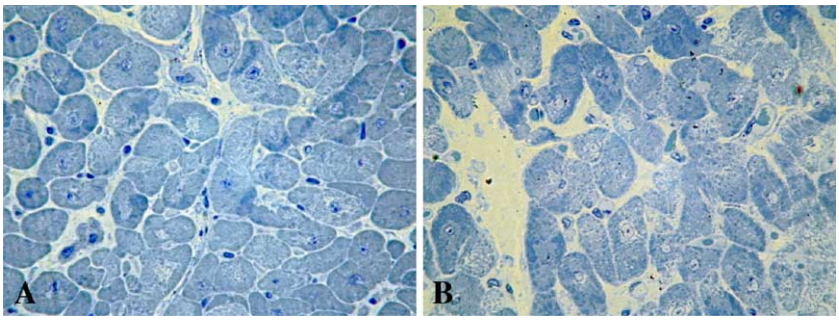

Fig. 3. Representative light microscopy images of toluidine-blue stained control (A) and 96 h volume overloaded heart (B) section. Cardiomyocytes from the volume overloaded heart show increased cross-sectional areas, suggestive of an hypertrophic response.

surgery (Fig. 2). At this time, the number of apoptotic cells had increased 50-fold from 0.72±0.15/mm^2 (control value) to 34.7±11.10/mm^2, corresponding to 12% of the total number of cardiomyocytes. Apoptotic cells observed at 24 h (19.9±5.96/mm^2) and at 96 h (10.9±5.36/mm^2) represented 6% and 4% of total cardiomyocytes, respectively. The increase in LMV, evident in overloaded hearts 96 h after surgery, was associated with the development of cellular hypertrophy (Fig. 3), as indicated by a significant enlargement in cardiomyocyte cross-section area (425.32±56.47 μm^2 relative to the control value of 225.31±32.69 μm^2; $P<0.05$) (Table 3).

3.4. Oxidative stress-induced signaling pathways for cardiomyocyte apoptosis and hypertrophy

To establish a possible relationship between MAPK activation and apoptotic and/or hypertrophic responses, we explored JNK and ERK phosphorylation status.

The phosphorylated active form of JNK increased significantly at 48 h of volume overload (Fig. 4), at the time of the greatest oxidative stress and when the largest number of apoptotic cells was evident. To clarify the death mechanism that is possibly involved in these effects, we examined the behaviour of caspase-9, which has a regulatory role in mitochondrial apoptotic pathways. Western blot analysis revealed that the catalytically active fragment of this enzyme was detectable at 24 h, with expression at 48 h of overload statistically significant (Fig. 5). At the same time, cytochrome *c* immunoreactivity was found to be increased in mitochondria-depleted cytosol (Fig. 6), suggesting its availability for the activation of procaspase-9. For caspase-3, the final effector of caspase cascade, we found that the levels of the 20 kDa active fragment of this enzyme increased in response to the overload, reaching a maximum value at 48 h (Fig. 7). This result was confirmed by direct measurements of caspase-3 catalytic activity (Table 4). No significant changes were observed over the entire study period for caspase-8 (Fig. 8).

The time course of ERK activation was quite different from that of JNK. Fig. 9 shows that the levels of the active, phosphorylated, form of ERK significantly increased, greater than 2-fold, at 96 h, coincident with the attenuation of oxidative stress and the appearance of a hypertrophic response.

Table 3
Cardiomyocyte cross-section area

	Control	24 h	48 h	96 h
μm^2	225.31±32.69	268.00±31.40	278.05±54.31	425.32±56.47*

* Significantly different ($P<0.05$) vs. Control.

4. Discussion

A possible involvement of oxidative stress in early biochemical changes associated with cardiac remodeling was explored in pig hearts subjected to volume overload by

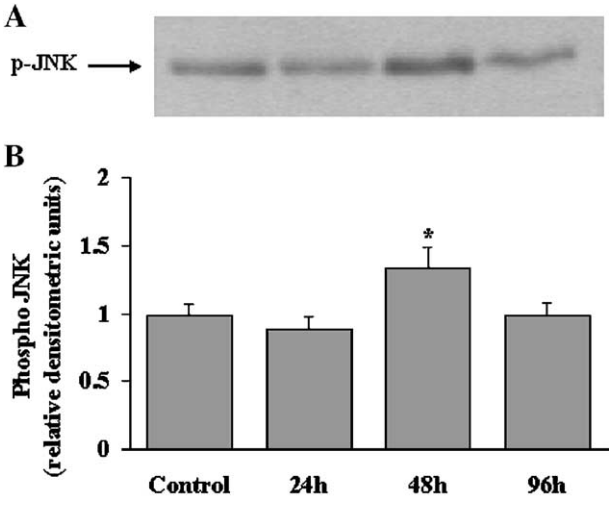

Fig. 4. JNK activation in control and volume overloaded heart. Equal amounts of cardiac homogenate proteins were separated in a 12% polyacrylamide gel and immunoblotted with a monoclonal antibody against the phosphorylated (activated) form of JNK. After stripping the membrane, polyclonal antibodies were used to detect total JNK protein level. (A) Representative immunoblot of phospho-JNK. B: quantitative data. Each bar represents the mean±S.E.M. of five different blots. Signals were quantified by densitometric analysis. The phospho-JNK densitometry values are expressed as relative densitometric units (densitometric unit, control phospho-JNK assumed=1) and were normalized with respect to JNK content. *Significant difference ($P<0.05$) from control.

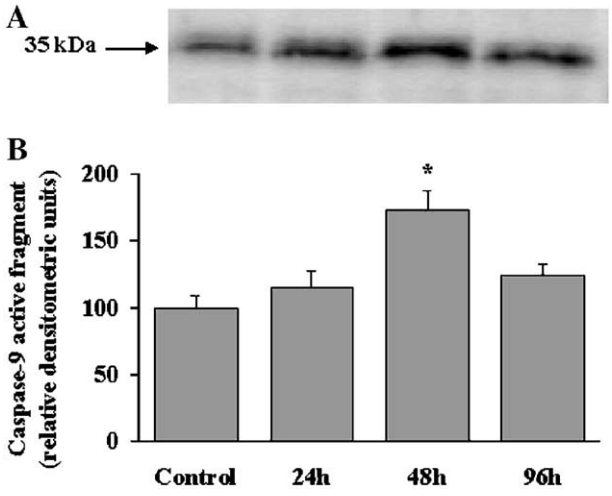

Fig. 5. Western blot analysis of caspase-9 active fragment in control and volume overloaded hearts. (A) Representative immunoblot. (B) Quantitative data. Each bar represents the mean ± S.E.M. of five different blots. Signals were quantified by densitometric analysis and are expressed as a percentage of the control. *Significant difference ($P < 0.05$) from control.

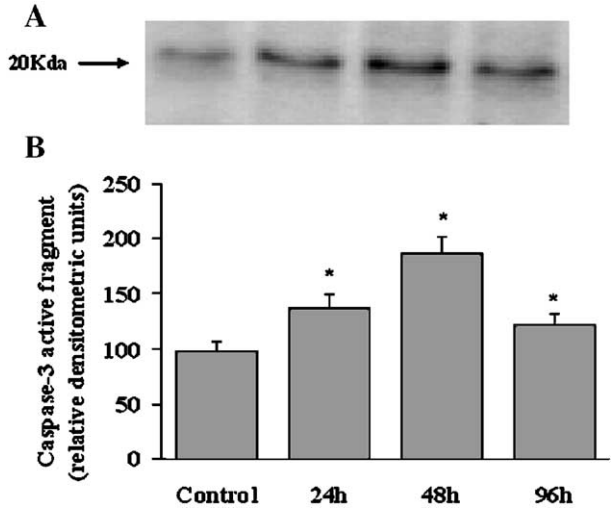

Fig. 7. Western blot analysis of caspase-3 active fragment in control and volume overloaded hearts. (A) Representative immunoblot. (B) Quantitative data. Each bar represents the mean ± S.E.M. of five different blots. Signals were quantified by densitometric analysis and are expressed as a percentage of the control. *Significant difference ($P < 0.05$) from control.

aortacaval shunt. The advantage of the pig heart model is its similar anatomo-functional characteristics with those of human heart. Moreover, the aortacaval shunt, as employed in this study, proved to be efficient in producing volume overload, as indicated by the hemodynamic data. The occurrence of oxidative stress under our experimental conditions was confirmed by the increase in a series of oxidative stress markers such as lipid peroxidation products, protein carbonyl content, and PARP activity, as a sign of oxidative DNA damage. A decrease in TAC, a measure of the overall free radical scavenging capacity, may be inversely related to the levels of ROS and possibly other reactive species. Marked signs of oxidative stress were observed at 48 h of overload, and persisted but considerably attenuated at 96 h. When compared to hemodynamic parameters, it becomes clear that the time course of oxidative stress parallels that of LVEDP, suggesting that mechanical strain is a major determinant of oxidative stress in overloaded hearts.

Several animal studies have suggested that mitochondria and xanthine oxidase may be significant contributors to ROS production in experimental heart failure [17]. In addition, clinical and animal studies indicate that a phagocyte-type NADPH oxidase complex, expressed in cardiomyocytes, may be a major source of ROS in pathological conditions [18,19]. NADPH oxidase is activated by several stimuli relevant to cardiovascular pathophysiology, including angiotensin II, noradrenalin, tumor necrosis factor-alpha and increased mechanical strain. In the latter case, NADPH activation might be regulated by FAS [20,21], a transmembrane receptor whose expression is upregulated in hearts subjected to volume overload [22,23].

Our results also indicate that myocyte apoptosis and hypertrophy play a significant part in early cardiac adaptation to acute volume overload, and that the temporal sequence of these events correlates with the development of oxidative stress. The wave of apoptosis observed during our study peaked at 48 h, coincident with the highest level of oxidative stress. When oxidative stress was significantly reduced at 96 h, hypertrophy was evident, consistent with

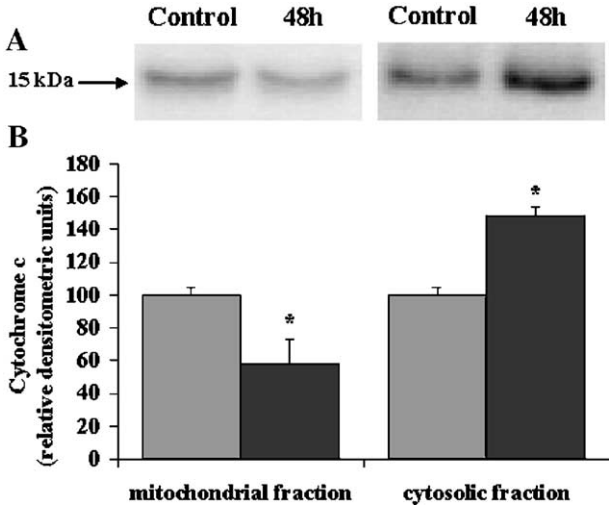

Fig. 6. Western blot analysis showing cytochrome *c* release from mitochondria. (A, C) Representative Western blot showing mitochondrial and cytosolic cytochrome *c* protein level in control and 48 h volume overloaded hearts. (B, D) Quantitative data. Each bar represents the mean value ± S.E.M. of five different blots. Signals were quantified by densitometric analysis and are expressed as a percentage of the control. *Significant difference ($P < 0.05$) from control.

Table 4
Caspase-3 activity

	Control	24 h	48 h	96 h
nmol pNA/h/mg protein	2.74 ± 0.16	3.82 ± 0.19*	5.23 ± 0.25*	3.58 ± 0.17*

* Significantly different ($P < 0.05$) vs. Control.

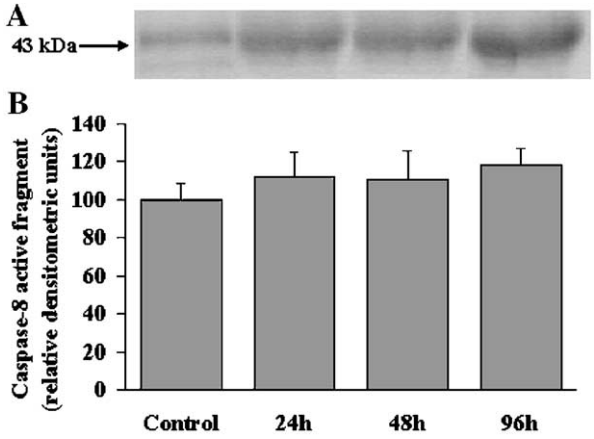

Fig. 8. Western blot analysis of caspase-8 active fragment in control and volume overloaded hearts. (A) Representative immunoblot. (B) Quantitative data. Each bar represents the mean±S.E.M. of five different blots. Signals were quantified by densitometric analysis and are expressed as a percentage of the control. No significant changes were observed for caspase-8 active fragment protein levels.

the view that in cardiac remodeling myocyte death or growth depends on the severity of oxidative stress.

To identify the underlying molecular mechanisms, we explored two possible signaling pathways, notably those involving the MAPKs, JNK and ERK [4,7,18], both regulated by oxidative stress and, respectively, pro- and antiapoptotic [4,7,23–25]. Based on the phosphorylation kinetics of these kinases, cardiomyocyte apoptosis was associated with an increase in JNK phosphorylation, in agreement with previous observations [26–29]. This activation was chiefly evident at 48 h from surgery, when both oxidative stress and the number of apoptotic cells reached their maximum. Furthermore, at 48 h of overload, the highest levels of JNK activation, coordinated with the release of cytochrome *c* from mitochondria and the maximum activation of caspase-9 and caspase-3. The observed mitochondrial release of cytochrome *c*, a process regulated by the Bcl-2 protein family [31,32], might be related to decreased Bcl-2 expression. In a recent study using the same experimental model [23], we found that Bcl-2 protein levels at 48 h of overload were reduced. Conversely, caspase-8, which is representative of the membrane receptor-mediated death pathway, showed no significant modification at any time. This observation agrees with a recent report [30] showing that cardiomyocytes contain significant levels of antagonist proteins, such cFLIP, that can prevent caspase-8 activation. The modest but significant increase in caspase-3 activity observed at 24 h of overload may involve an additional JNK-independent apoptotic pathway, represented by the endo/sarcoplasmic reticulum (ER/SR)-induced cell death pathway. Alterations in Ca^{2+} homeostasis and increases in ROS production can cause ER/SR stress with the release and the consequent activation of caspase-12 [33]. Although the downstream targets of caspase-12 are yet to be understood, recent studies [34] suggest a possible activation of caspase-3. As we reported previously, our experimental conditions induced a significant alteration in Ca^{2+} homeostasis [23]. This, joined with oxidative stress, could trigger the activation of caspase-12. Overall, our findings support the view that a mitochondrial pathway is the principal factor in cardiomyocyte apoptosis associated with oxidative stress-induced imbalance between the activation rates of JNK and ERK. Similar results have been reported in recent studies on cultured cardiomyocytes [35], and our in vivo observations are the first in an animal model of cardiac overload.

The hypertrophic response that appeared in overloaded hearts at 96 h after surgery coincided with a reduction in oxidative stress, an effect that might be related to an attenuation of mechanical strain on the ventricle wall. This is consistent with the observed recovery of cardiac functional parameters which, based on our previous results [23], is at least partly due to restored efficiency of sarcoplasmic reticulum calcium pumping. The marked increase in ERK phosphorylation found at the same time suggests that this redox-sensitive kinase is involved in the hypertrophic response. Although the mechanisms accounting for selective ERK activation by mild oxidative stress (and its potential inactivation by overt oxidative stress) are not defined, these results agree with several reports [17,36,37] indicating that in intact heart and in isolated cardiomyocytes, the ERK pathway is implicated, through the activation of transcription specific factors, in protection against apoptosis and in hypertrophic growth.

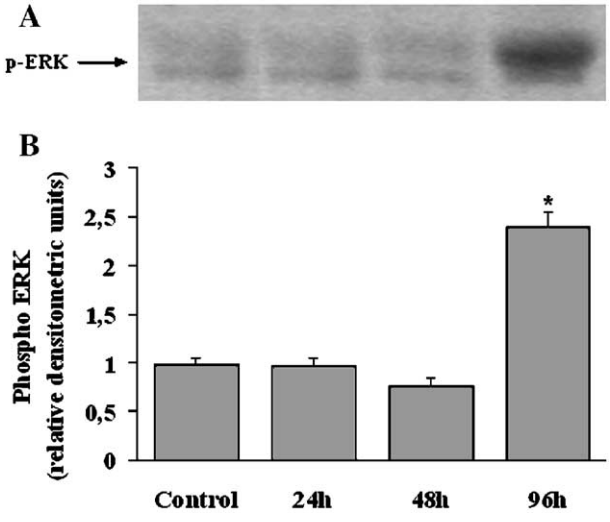

Fig. 9. ERK activation in control and volume overloaded hearts. Equal amounts of cardiac homogenate proteins were separated in a 12% polyacrylamide gel and immunoblotted with specific polyclonal antibodies against the phosphorylated (activated) form of ERK. After stripping, the membrane polyclonal antibodies were used to detect total ERK protein level. (A) Representative immunoblot of phosho-ERK. Each bar represents the mean±S.E.M. of five different blots. Signals were quantified by densitometric analysis. The phospho-ERK densitometry values are expressed as relative densitometric units (densitometric unit, control phospho-ERK assumed=1) and were normalized with respect to ERK content. *Significant difference ($P<0.05$) from control.

We conclude that an early and transient oxidative stress which occurs within hours after heart muscle is subjected to volume overload may mediate amplitude-dependent apoptotic and hypertrophic responses in cardiomyocytes through the selective activation of redox-sensitive JNK and ERK. Future studies can confirm this proposal by the use of antioxidants and selective MAPKs inhibitors. Both the source of ROS in the overloaded hearts and the molecular mechanisms leading to the activation of different kinases depending on the intensity of oxidative stress must be explored. We believe that further studies have potential value in suggesting prompt and suitable interventions to prevent cardiac dysfunction associated with hemodynamic overload.

Acknowledgements

We are grateful to Prof. Alan Levine for careful review of the manuscript. We also thank Valentina Vitale for her skilled assistance. This study was supported by a financial grant from Ente Cassa di Risparmio di Firenze.

References

[1] M. Maytin, W.S. Colucci, Molecular and cellular mechanisms of myocardial remodelling, J. Nucl. Cardiol. 9 (2002) 319–327.
[2] A.K. Dhalla, M.F. Hill, P.K. Singal, Role of oxidative stress in transition of hypertrophy to heart failure, J. Am. Coll. Cardiol. 28 (1996) 506–514.
[3] D. Cesselli, I. Jakoniuk, L. Barlucchi, A.P. Beltrami, T.H. Hintze, B. Nadal-Ginard, J. Kajstura, A. Leri, P. Anversa, Oxidative stress-mediated cardiac cell death is a major determinant of ventricular dysfunction and failure in dog dilated cardiomyopathy, Circ. Res. 89 (2001) 279–286.
[4] D.B. Sawyer, D.A. Siwik, L. Xiao, D.R. Pimentel, K. Singh, W.S. Colucci, Role of oxidative stress in myocardial hypertrophy and failure, J. Mol. Cell. Cardiol. 34 (2002) 379–388.
[5] D.A. Siwik, J.D. Tzortzis, D.R. Pimental, D.L.-F. Chang, P.J. Pagano, K. Singh, D.B. Sawyer, W.S. Colucci, Inhibition of copper-zinc superoxide dismutase induces cell growth, hypertrophic phenotype, and apoptosis in neonatal rat cardiac myocyte in vitro, Circ. Res. 85 (1999) 147–153.
[6] D.R. Pimentel, J.K. Amin, T. Miller, J. Viereck, J. Oliver-Krasinki, R. Baliga, J. Wang, D.A. Siwik, K. Singh, P. Pagano, W.S. Colucci, D.B. Sawyer, Reactive oxygen species mediate amplitude-dependent hypertrophic and apoptotic responses to mechanical stretch in cardiac myocytes, Circ. Res. 89 (2001) 453–460.
[7] F. Qin, J. Shite, C.-S. Liang, Antioxidants attenuate myocyte apoptosis and improve cardiac function in CHF: association with changes in MAPK pathways, Am. J. Physiol.: Heart Circ. Physiol. 285 (2003) H822–H832.
[8] P.A. Modesti, S. Vanni, I. Bertolozzi, I. Cecioni, G. Polidori, R. Paniccia, B. Bandinelli, A. Perna, P. Liguori, M. Boddi, G. Galanti, G.G. Serneri, Early sequence of cardiac adaptations and growth factor formation in pressure- and volume-overload hypertrophy, Am. J. Physiol.: Heart Circ. Physiol. 279 (2000) H976–H985.
[9] D.J. Sahn, A. De Maria, J. Kisslo, A. Weyman, Recommendations regarding quantitation in M-mode echocardiography: results of a survey of echocardiographic measurements, Circulation 58 (1978) 1072–1083.
[10] M.P. Feneley, J.W. Gaynor, G.W. Maier, S.A. Gall Kisslo Jr., J.S. Rankin, In vivo estimation of left ventricular wall volume in volume-overloaded canine hearts, Am. J. Physiol.: Heart Circ. Physiol. 255 (1988) H1399–H1404.
[11] M.M. Bradford, A rapid and sensitive method for the quantitation of microgram quantities of protein utilizing the principle of protein dye binding, Anal. Biochem. 72 (1976) 248–254.
[12] H. Esterbauer, R.J. Schaur, H. Zollner, Chemistry and Biochemistry of 4-hydroxynonenal, malonaldehyde and related aldehydes, Free Radic. Biol. Med. 11 (1991) 81–128.
[13] R.L. Levine, J.A. Williams, E.R. Stadtman, E. Shacter, Carbonyl assays for determination of oxidatively modified proteins, Methods Enzymol. 233 (1994) 346–357.
[14] E.B. Affar, P. Duriez, R.G. Shah, F.R. Sallmann, S. Bourassa, J.H. Kupper, A. Burkle, G.G. Poirier, Immunodot blot method for the detection of poly(ADP-ribose) synthesized in vitro and in vivo, Anal. Biochem. 259 (1998) 280–283.
[15] T.L. Yue, C. Wang, A.M. Romanic, K. Kikly, P. Keller, W.E. De Wolf Jr., T.K. Hart, H.C. Thomas, B. Storer, J.L. Gu, X. Wang, G.Z. Feuerstein, Staurosporine-induced apoptosis in cardiomyocytes: a potential role of caspase-3, J. Mol. Cell. Cardiol. 30 (1998) 495–507.
[16] J.H. Wijsman, R.R. Jonker, R. Keijzer, C.J.H. Van de Velde, C.J. Cornelisse, J.H. Van Dierendonck, A new method to detect apoptosis in paraffin sections: in situ end-labeling of fragmented DNA, J. Histochem. Cytochem. 41 (1993) 7–12.
[17] C. Heymes, J.K. Bendall, P. Ratajczak, A.C. Cave, J.L. Samuel, G. Hasenfuss, A.M. Shah, Increased myocardial NADPH oxidase activity in human heart failure, J. Am. Coll. Cardiol. 41 (2003) 2164–2171.
[18] J.M. Li, N.P. Gall, D.J. Grieve, M. Chen, A.M. Shah, Activation of NADPH oxidase during progression of cardiac hypertrophy to failure, Hypertension 40 (2002) 477–484.
[19] K.K. Griendling, D. Sorescu, M. Ushio-Fukai, NAD(P)H oxidase: role in cardiovascular biology and disease, Circ. Res. 86 (2000) 494–501.
[20] Y. Suzuki, Y. Ono, Y. Hirabayashi, Rapid and specific oxygen species generation via NADPH oxidase activation during Fas-mediated apoptosis, FEBS Lett. 425 (1998) 209–212.
[21] S. Devadas, J. Hinshaw, L. Zaritskaya, M.S. Williams, Fas-stimulated generation of reactive oxygen species or exogenous oxidative stress sensitive cells to Fas-mediated apoptosis, Free Radic. Biol. Med. 35 (2003) 648–661.
[22] K.C. Wollert, J. Heineke, J. Westermann, M. Ludde, B. Fiedler, W. Zierhut, D. Laurent, M.K. Bauer, K. Schulze-Osthoff, H. Drexler, The cardiac Fas (APO-1/CD95) receptor/Fas ligand system. Relation to diastolic wall stress in volume-overload hypertrophy. In vivo and activation of the transcription factor AP-1 in cardiac myocytes, Circulation 101 (2000) 1172–1178.
[23] C. Nediani, A. Celli, L. Formigli, A.M. Perna, C. Fiorillo, V. Ponziani, Possible role of acylphosphatase, Bcl-2 and Fas/Fas-L system in the early changes of cardiac remodeling induced by volume overload, Biochim. Biophys. Acta 1638 (2003) 217–226.
[24] R. Aikawa, I. Komuro, T. Yamazaki, Y. Zou, S. Kudoh S., M. Tanaka Shiojima I., Y. Hiroi, Y. Yazaki, Oxidative stress activates extracellular signal-regulated kinases through Src and Ras in cultured cardiac myocytes of neonatal rats, J. Clin. Invest. 100 (1997) 1813–1821.
[25] T.L. Yue, C. Wang, J.L. Gu, X.L. Ma, S. Kumar, J.C. Lee, G.Z. Feuerstein, H. Thomas, B. Maleeff, E.H. Ohlstein, Inhibition of extracellular signal-regulated kinase enhances ischemia/reoxygenation-induced apoptosis in cultured cardiac myocytes and exaggerates reperfusion injury in isolated perfused heart, Circ. Res. 86 (2000) 692–699.
[26] G.Z. Feuerstein, P.R. Young, Apoptosis in cardiac diseases: stress- and mitogen-activated signaling pathways, Cardiovasc. Res. 45 (2000) 560–569.
[27] N.A. Turner, F. Xia, G. Azhar, X. Zhang, L. Liu, J.Y. Wei, Oxidative stress induces DNA fragmentation and caspase activation via the c-Jun

NH2-terminal kinase pathways in H9c2 cardiac muscle cells, J. Mol. Cell. Cardiol. 30 (1998) 1789–1801.
[28] W.G. Li, A. Zaheer, L. Coppey, H.J. Oskarsson, Activation of JNK in the remote myocardium after large myocardial infarction in rats, Biochem. Biophys. Res. Commun. 246 (1998) 816–820.
[29] M. Sato, D. Bagchi, A. Tosaki, D.K. Das, Grape seed proanthocyanidin reduces cardiomyocyte apoptosis by inhibiting ischemia/reperfusion-induced activation of JNK-1 and c-Jun, Free Radic. Biol. Med. 31 (2001) 729–737.
[30] T. Imanishi, C.E. Murry, H. Reinecke, T. Hano, I. Nishio, W.C. Liles, L. Hofsta, K. Kim, K.D. O'Brien, S.M. Schwartz, D.K. Han, Cellular FLIP is expressed in cardiomyocytes and down-regulated in TUNEL-positive grafted cardiac tissues, Cardiovasc. Res. 48 (2000) 101–110.
[31] J. Cai, D.P. Jones, Superoxide in apoptosis. Mitochondrial generation triggered by cytochrome *c* loss, J. Biol. Chem. 273 (1998) 11401–11404.
[32] J. Yang, X. Liu, K. Bhalla, C. Kim, A.M. Ibrado, J. Cai, T.I. Peng, D.P. Jones, X. Wang, Prevention of apoptosis by Bcl-2: release of cytochrome *c* from mitochondria blocked, Science 275 (1997) 1129–1130.
[33] T. Nakagawa, H. Zhu, N. Morishima, E. Li, J. Xu, B.A. Yankner, J. Yuan, Caspase-12 mediates endoplasmic-reticulum-specific apoptosis and cytotoxicity by amyloid-beta, Nature 403 (2000) 98–103.
[34] A.J. Dirks, C. Leeuwenburgh, Aging and lifelong calorie restriction result in adaptations of skeletal muscle apoptosis repressor, apoptosis-inducing factor, X-linked inhibitor of apoptosis, caspase-3, and caspase-12, Free Radic. Biol. Med. 36 (2004) 27–39.
[35] H. Aoki, P.M. Kang, J. Hampe, K. Yoshimura, T. Noma, M. Matsuzaki, S. Izumo, Direct activation of mitochondrial apoptosis machinery by c-Jun N-terminal kinase in adult cardiac myocytes, J. Biol. Chem. 277 (2002) 10244–10250.
[36] R. Schulz, S. Aker, S. Belosjorow, I. Konietzka, U. Rauen, G. Heusch, Stress kinase phosphorylation is increased in pacing-induced heart failure in rabbits, Am. J. Physiol.: Heart Circ. Physiol. 285 (2003) H2084–H2090.
[37] L. Xiao, D.R. Pimentel, J. Wang, K. Singh, W.S. Colucci, D.B. Sawyer, Role of reactive oxygen species and NAD(P)H oxidase in alpha(1)-adrenoceptor signaling in adult rat cardiac myocytes, Am. J. Physiol.: Cell Physiol. 282 (2002) C926–C934.